

Bunch Length and Impedance Measurements in SPEAR*

K. BANE, M. DONALD, A. HOFMANN^a, J. JOWETT^a, W. LOCKMAN^b
P. MORTON, R. STEGE, W. SPENCE, P. WILSON

Stanford Linear Accelerator Center
Stanford University, Stanford, California, 94309

Abstract

Subsequent to an extensive smoothing of the vacuum chamber a comprehensive study of the SPEAR impedance was undertaken. Bunch length, synchrotron quadrupole mode frequency, and parasitic mode loss were measured as functions of beam current. The results showed that, although the gross longitudinal impedance had indeed been reduced, the 'capacitive' component had also decreased relative to the 'inductive'—to the extent that previously compensated potential well distortion now induced bunch lengthening at low currents, and the turbulent threshold had actually been lowered. A specially designed multi-cell disc-loaded 'capacitor' cavity was shown to be capable of removing this effect by restoring the original compensation. A model of the new SPEAR impedance is also obtained.

In the summer of 1983 the SPEAR II vacuum chamber was extensively rebuilt with the aim of reducing the impedance, which had then been well-understood for some time.¹ The 1984-85 high energy physics run commenced with the commissioning of new 'mini- β ' interaction region insertions from which the expected luminosity enhancement was not realized. This provoked a comprehensive machine study of impedance driven effects, in light of the rebuilt vacuum chamber, which might contribute to limit the luminosity—on which we now report.

The SPEAR 'Capacitor'

Inductive storage ring vacuum chamber components are elements such as steps, shallow cavities and bellows that tend to lengthen the bunch as the beam current is increased. The average slope of the induced voltage is opposite in sign to the slope of the rf wave, therefore reducing the slope seen by the particles. Capacitive vacuum chamber components are elements such as deep cavities that tend to shorten the bunch with current since the slope of the induced voltage has the same sign as the rf wave. Whether an object is inductive or capacitive depends critically on the length of the driving charge—vacuum chamber objects tending to appear more capacitive for shorter bunches while to a sufficiently long bunch even a deep cavity will appear inductive.

In old SPEAR II the balance of inductive and capacitive vacuum chamber components was tilted slightly toward the latter at the nominal bunch length—at low currents the bunch length actually decreased¹ with current. In the changes made to the vacuum chamber in 1983 mostly large, capacitive objects were removed—such as two PEP 5-cell rf cavities—leaving the machine more inductive and resulting in increased bunch lengthening. Built before the impact of vacuum chamber discontinuities on an electron ring's performance was fully appreciated, SPEAR contains many untapered changes in vacuum chamber cross-section. Probably the dominant contributors to the ring's impedance, the inductive nature of SPEAR could be reduced by smoothing them—an enormous undertaking. Instead we attempted to achieve the same effect on bunch lengthening by adding a capacitive device to the ring. The use of a special insertion to modify the reactive impedance of a storage ring has been previously discussed by Briggs and Neil² and a

capacitive device was once installed in the CERN ISR for the same purpose.³

SPEAR has 2 meters of free straight section centered on an unused interaction region. Our exercise was to design a device that is as capacitive as possible and that will fit in these 2 m. An important constraint on the design is that the device may not cut into the beam stay-clear region—a cone that has a minimum radius of 1 cm at the interaction point, and that flares out to 7 cm at each end of the 2 m space. We investigate the properties of structures that seem likely to be good 'capacitors'—two variants of a periodic sequence of deep cylindrically symmetric cavities—using the program TBCI.⁴ We compare the results to those for 15 PEP rf cells which we estimate to have an impedance equivalent to what was removed from the ring.

'Capacitor' Design: An indicator of the capacitive or inductive character of a device is the average slope of the longitudinal wakefield in the core of a gaussian driving charge. We define the capacitance parameter

$$\alpha = \sigma_z \frac{\int_{-\sigma_z}^{\sigma_z} W'_z(s) e^{-s^2/2\sigma_z^2} ds}{\int_{-\sigma_z}^{\sigma_z} e^{-s^2/2\sigma_z^2} ds}, \quad (1)$$

with σ_z the bunch length and $W'_z(s)$ the slope of the longitudinal wake at position s within the bunch. If we choose a positive value of the wakefield to signify energy loss and the bunch is moving in the $-s$ direction, $\alpha > 0$ for a capacitive wake and $\alpha < 0$ for an inductive wake.

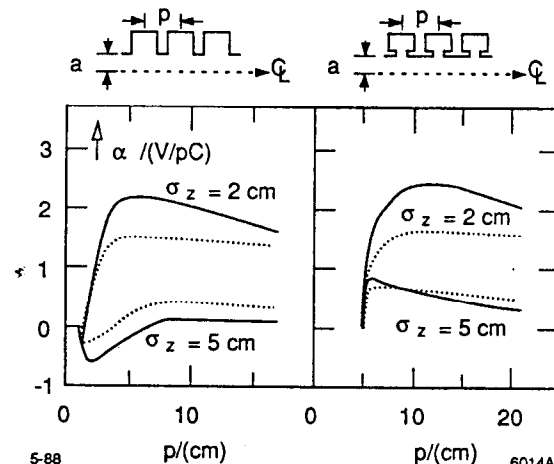


Fig. 1. The parameter α for 2 m of a periodic structure with simple irises (left plot) and one with reentrant irises (right), as a function of structure period p , for bunch lengths of 2 cm and 5 cm. The cavity geometry is sketched at the top. Results are given for iris radius $a = 3.5$ cm (the solid lines) and for $a = 5.0$ cm (the dots).

Consider the two periodic, cylindrically symmetric structures that are sketched at the top of Fig. 1—a simple disk-loaded structure and a periodic reentrant cavity structure. In order to be most effective as capacitors we will avoid contributions from the outer cavity walls that make the wakefield more inductive by keeping them a sufficient distance from the structure axis for all combinations of parameters that we present so that no wave generated by the head of the beam reflects back

* Work supported by the United States Department of Energy, contract DE-AC03-76SF00515.

^a CERN, Geneva 23, Switzerland

^b University of California, Santa Cruz, Ca. 95064, U.S.A.

in time to affect the tail. For both devices the walls separating the cavities are 1 cm thick; in the reentrant cavity design the iris protrusions are 0.8 cm thick and extend 2 cm into the cavity. The beam sees only a smooth tube when the period p is 1 cm for the disk-loaded structure and when $p = 5$ cm for the reentrant cavity structure. We compare the capacitance of 2 m of these structures with that of 15 PEP rf cells. A PEP cell is a deep, reentrant cavity with an iris radius of 5 cm; the total length of 15 PEP cells is 6 m.

The plots of Fig. 1 show the dependence of α —as computed by TBCI—on the period length p of our two example structures, for $\sigma_z = 2$ cm and 5 cm. In general α tends to rise to a maximum as p increases, and then to level off or decrease gradually. A significant difference between the effect of the two structures is that α is negative for the disk-loaded structure when the gap is small, but is always positive for the reentrant cavity. α depends strongly on bunch length in both cases, decreasing as the bunch length increases. At the short bunch length α also decreases as the iris aperture a is increased; however, at the longer bunch length its dependence on aperture is not very pronounced. The reentrant cavity makes the better capacitor over the parameter range explored. At $\sigma_z = 2$ cm and with $a = 3.5$ cm the peak value of α is 2.5, (at $p = 6$ cm), for the reentrant cavity whereas the peak value is 2.2, ($p = 12$ cm), for the disk-loaded structure. $\alpha = 2.5$ for 15 PEP cells at the same bunch length.

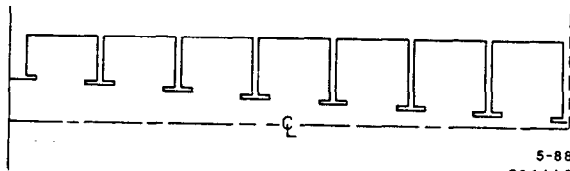


Fig. 2. The left half of the SPEAR capacitor. The right half is given by the reflection of this figure about the dashed line at the right.

The device that was built and temporarily installed in the ring—which we call the ‘SPEAR capacitor’, shown in Fig. 2—is our reentrant structure with 14 cells but with iris apertures tapered (from a minimum a of 1.2 cm at the interaction point to a maximum of 7.5 cm at the ends) to hug the luminosity stay clear cone in order to maximize its effect. The capacitor was fabricated from 31.5 cm ID stainless steel tubing into which irises of magnetic stainless steel (chosen to damp cavity modes and avoid multimode effects) were brazed.

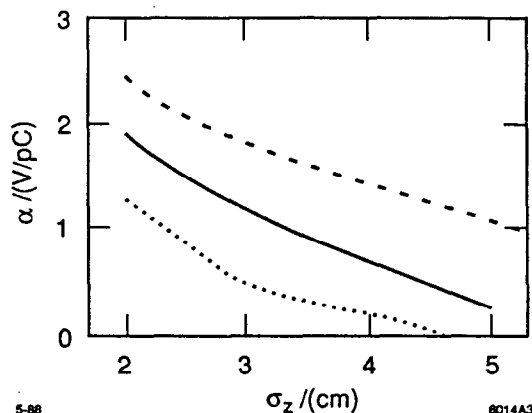


Fig. 3. The capacitance parameter α as a function of bunch length σ_z for the 14 cell capacitor (the solid line), for 15 PEP rf cells (dashes), and for a 22 cell disk-loaded structure (dots).

Fig. 3 shows that α decreases much slower with σ_z for the PEP cells than for the capacitor—at $\sigma_z = 2$ cm the capacitor is 75% as effective as 15 PEP cells, whereas at $\sigma_z = 5$ cm it is only 25% as effective. In order to make the capacitor more effective we need to increase its length and/or reduce the iris apertures.

The results shown for the simple disk-loaded structure include the iris apertures tapered to follow the stay clear.

New SPEAR II Impedance

Bunch length measurements were performed using a IMA-CON 500 streak camera, calibrating its time base by filling two adjacent buckets in SPEAR. Gathering sufficient synchrotron light at low currents (≈ 0.5 mA) requires reducing the collimation such that a resolution of only 2.4 cm (comparable to the natural bunch length at nominal rf voltages) is achieved—otherwise the resolution (which adds in quadrature to the actual bunch length) is a quite tolerable 1.2 cm. Each measurement we report represents an average of 10 separate observations—the associated errors signify one standard deviation about the mean.

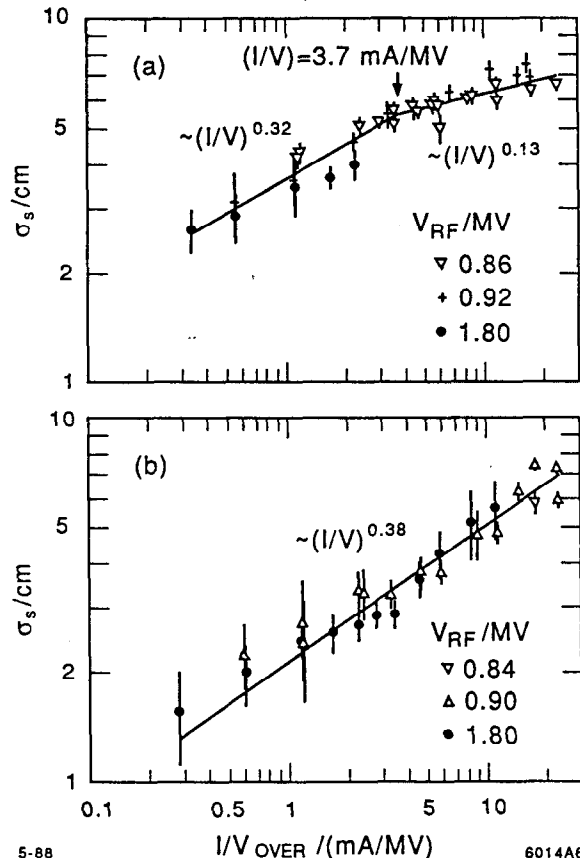


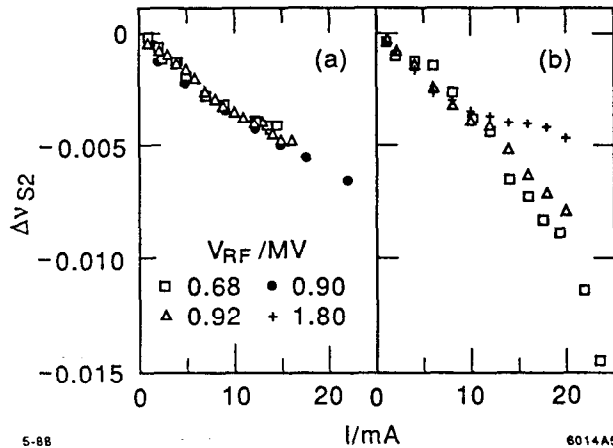
Fig. 5. Bunch length measured by a streak camera vs. the Chao-Gareyte variable in which scaling is expected above the turbulent threshold. a) New SPEAR II. b) New SPEAR II including the capacitor—exhibiting a reduced bunch length.

The totality of such measurements are shown in Fig. 5 in which use is made of the (single machine) scaling variable⁵

$$\frac{I}{V_{\text{over}}} = \frac{\alpha_p h I}{2\pi E \nu_s^2} \quad (2)$$

where the over-voltage $V_o = [V_{\text{RF}}^2 - (\text{energy loss per turn}/e)^2]^{1/2}$, α_p is the momentum compaction, h the harmonic number, E the beam energy, and ν_s the incoherent synchrotron tune at beam current $I = 0$. For SPEAR at $E = 2.07$ GeV the radiative energy loss per turn = 125 keV and the contribution of parasitic mode losses at the currents studied ≤ 10 keV so that practically $V_o \approx V_{\text{RF}}$. Scaling in I/V_o is characteristic of turbulent or mode-coupling instability driven bunch lengthening⁶ and is expected to break down at sufficiently low currents where the dominance of pure quantum fluctuations, possibly accompanied by potential well distortion, sets in—i.e., points corresponding to different V_o/E^3 will lie on different curves, the

locations at which they depart from the scaling curve representing the turbulent threshold. The data in both cases are consistent with turbulent scaling over the entire range of parameters studied which included a variation in V_{RF} of well over a factor of two. This indicates that the turbulent threshold may occur at quite low current though it is not possible to rule out some scaling violation associated with potential well distortion engendered bunch lengthening toward the lower I/V_0 range of the data. That this may indeed be the case is suggested by the observation of a discontinuous change in slope in the dependence of the beam centroid phase (relative to the rf phase) on current for $I/V_0 \cong 1.9 \text{ mA/MV}$ at $V_0 = 0.77 \text{ MV}$ and $E = 1.55 \text{ GeV}$. After the installation of the capacitor a similar kink was seen for $I/V_0 \cong 3.3 \text{ mA/MV}$ at $V_0 = 1.81 \text{ MV}$ and $E = 2.07 \text{ GeV}$. This may be contrasted with the old SPEAR II measurement of a kink at $I/V_0 \cong 3.9 \text{ mA/MV}$ at $V_0 = 0.77 \text{ MV}$ and $E = 1.55 \text{ GeV}$.



5-88
Fig. 6. Shift in the frequency of the quadrupole mode $\Delta\nu_{s2} = \nu_{s2} - 2\nu_{s1}$. a) New SPEAR II. b) New SPEAR II including the capacitor.

The data are well parameterized by

$$\sigma_z \cong 3.63 \text{ cm} \left(\frac{I \text{ MV}}{V_0 \text{ mA}} \right)^{0.32}, \quad \frac{I}{V_0} \leq 3.72 \frac{\text{mA}}{\text{MV}} \quad (3)$$

$$\sigma_z \cong 4.64 \text{ cm} \left(\frac{I \text{ MV}}{V_0 \text{ mA}} \right)^{0.13}, \quad \frac{I}{V_0} \geq 3.72 \frac{\text{mA}}{\text{MV}} \quad (4)$$

prior to the installation of the capacitor, and by

$$\sigma_z \cong 2.14 \text{ cm} \left(\frac{I \text{ MV}}{V_0 \text{ mA}} \right)^{0.38} \quad (5)$$

with the capacitor in the ring. Old SPEAR II has been described by¹

$$\sigma_z \cong 0.591 \text{ cm} \left(\frac{I \text{ MV}}{V_0 \text{ mA}} \right)^{0.76}, \quad \frac{I}{V_0} \geq 4.0 \frac{\text{mA}}{\text{MV}} \quad (6)$$

The same general scaling argument⁵ that lead to the scaling variable then tells us the behavior of the reactive component of the longitudinal impedance function

$$Z_I \sim \omega^{1.17}, \quad \omega \gtrsim (2\pi)870 \text{ MHz} \quad (7)$$

$$Z_I \sim \omega^{5.70}, \quad \omega \lesssim (2\pi)870 \text{ MHz} \quad (8)$$

before the capacitor, and

$$Z_I \sim \omega^{0.66} \quad (9)$$

including the capacitor, over all frequencies sampled by the bunch. Both differ significantly from the old SPEAR II behavior

$$Z_I \sim \omega^{-0.68} \quad (10)$$

To gain additional information on the reactive impedance, measurements were also performed of the shift with current in the frequency of artificially excited single bunch coherent

quadrupole oscillations

$$\Delta\nu_{s2} = \nu_{s2} - 2\nu_{s1} \quad (11)$$

where ν_{s1} is the (essentially unshifted) coherent dipole frequency. The data, taken at $E = 2.07 \text{ GeV}$ displayed in Fig. 6 are well described for small currents by

$$\Delta\nu_{s2} \approx (-4.5 \pm 0.5) \times 10^{-4} \frac{I}{\text{mA}}, \quad I \lesssim 5 \text{ mA} \quad (12)$$

independent of V_{RF} and showing no measurable dependence on the presence of the capacitor. The small current behavior is most sensitive to the high frequency nature of the impedance, and the fact that the absolute slope with current of the shift is seen to decrease with increasing current (increasing bunch length) is qualitatively consistent with the monotone decreasing behavior of the impedance toward lower frequencies inferred from the bunch length measurements. To be more quantitative we consider the impedance function smeared over the form factor of the bunch

$$\langle Z_I \rangle_{1/\sigma_z} \equiv \sigma_z^2 \int_{-\infty}^{\infty} d\omega \omega Z_I(\omega) \frac{e^{-\omega^2/2\sigma_z^2}}{\sqrt{2\pi}} \quad (13)$$

which we regard as a function of $\omega = 1/\sigma_z$ and which is closely related to the capacitance parameter of the previous section. Then for small values of the current⁶

$$\langle Z_I \rangle_{1/\sigma_z} \cong 4\sqrt{2\pi} \omega_{\text{rev}}^2 \frac{E}{e\alpha_p} \nu_s \sigma_z^2 \frac{\Delta\nu_{s2}}{I} \quad (14)$$

where it is assumed that the quadrupole frequency shift is reduced to about 1/2 the small amplitude incoherent synchrotron frequency shift by the charge density decreasing effects of the quadrupole oscillations themselves.⁷ At small currents $\sigma_z \sim 1/\nu_s$ as V_{RF} varies so that the observed constancy of the quadrupole frequency shift implies that the impedance is changing in direct proportion to the bunch length over the range of the data (wherein it changes by about 60%), or

$$\langle Z_I \rangle_{\omega} \cong 3810 \frac{\Omega}{\text{turn}} \left(\frac{\omega}{(2\pi)1560 \text{ MHz}} \right)^{-1}, \quad \omega \gtrsim (2\pi)1560 \text{ MHz} \quad (15)$$

out to at least about 2500 MHz—which is not completely dissimilar from old SPEAR II, albeit commencing at somewhat higher frequencies. The capacitor appears to have little effect in this high frequency domain, consistent with the expectation $\Delta(\Delta\nu_{s2})_{15 \text{ PEP cells}} \approx 0.5 \times 10^{-4} I/\text{mA}$.

Our overall semi-quantitative picture of the new SPEAR II reactive impedance prior to the introduction of the capacitor is then that at low frequencies ($\omega \approx (2\pi)730 \text{ MHz}$) it is a very rapidly increasing function of frequency (7), slowing considerably at $\omega \approx (2\pi)900 \text{ MHz}$ but continuing to increase (not too much faster than a simple inductor or broad-band resonator) and then to undergo a rapid turnover so as to reach, by $\omega \approx (2\pi)1560 \text{ MHz}$ a régime in which it decreases $\sim \omega^{-1}$ around a rather modest absolute magnitude (15). The addition of the capacitor successfully modified this behavior—for $\omega \gtrsim (2\pi)730 \text{ MHz}$ starting from about the same magnitude the rapid rise was dramatically slowed (9) such that at $\omega \approx (2\pi)950 \text{ MHz}$ (from the ratio of the bunch lengths) Z_I becomes roughly 3.5 times smaller.

1. P. B. Wilson et al., *IEEE Trans. Nucl. Sci.*, NS-24(1977)1211.
2. R. Briggs and V. Neil, *Plasma Physics*, 8(1966)255.
3. P. Bramham et al., *ISR-GS/RF-AH/amb*, CERN, 1976.
4. T. Weiland, *DESY 82-015* (1982) and *Nucl. Inst. Meth.*, 212(1983)13.
5. A. Chao and J. Gareyte, *SPEAR-197/PEP-224*, SLAC, 1976.
6. A. W. Chao, *Physics of High Energy Particle Accelerators*, American Institute of Physics, New York, 1982, gives a general review.
7. S. Hansen et al., *IEEE Trans. Nucl. Sci.*, NS-22(1975)1381.